Plant Reproduction
https://doi.org/10.1007/s00497-023-00468-5

ORIGINAL ARTICLE

Disruption of pollen tube homogalacturonan synthesis relieves pollen tube penetration defects in the Arabidopsis *O-FUCOSYLTRANSFERASE1* mutant

Kayleigh J. Robichaux[1] · Devin K. Smith[1] · Madison N. Blea[1] · Chrystle Weigand[1] · Jeffrey F. Harper[1] · Ian S. Wallace[1]

Received: 21 November 2022 / Accepted: 5 May 2023
© The Author(s), under exclusive licence to Springer-Verlag GmbH Germany, part of Springer Nature 2023

Abstract

During angiosperm sexual reproduction, pollen tubes must penetrate through multiple cell types in the pistil to mediate successful fertilization. Although this process is highly choreographed and requires complex chemical and mechanical signaling to guide the pollen tube to its destination, aspects of our understanding of pollen tube penetration through the pistil are incomplete. Our previous work demonstrated that disruption of the *Arabidopsis thaliana O-FUCOSYLTRANSFERASE1 (OFT1)* gene resulted in decreased pollen tube penetration through the stigma–style interface. Here, we demonstrate that second site mutations of Arabidopsis *GALACTURONOSYLTRANSFERASE 14 (GAUT14)* effectively suppress the phenotype of *oft1* mutants, partially restoring silique length, seed set, pollen transmission, and pollen tube penetration deficiencies in navigating the female reproductive tract. These results suggest that disruption of pectic homogalacturonan (HG) synthesis can alleviate the penetrative defects associated with the *oft1* mutant and may implicate pectic HG deposition in the process of pollen tube penetration through the stigma–style interface in Arabidopsis. These results also support a model in which OFT1 function directly or indirectly modifies structural features associated with the cell wall, with the loss of *oft1* leading to an imbalance in the wall composition that can be compensated for by a reduction in pectic HG deposition.

Keywords Pollen-pistil interaction · Cell wall · Pectin deposition · Glycosyltransferase · O-fucosylation

Introduction

Double fertilization in angiosperms requires precise communication between male and female gametes (Johnson et al. 2019). Plant sperm cells are nonmotile and must be transported to the distant egg cell-containing ovule via a specialized structure called the pollen tube. Upon interaction with stigmatic papillar cells, pollen grains germinate to form a pollen tube, which subsequently and sequentially invades the stigmatic papillar cell, the style, and the transmitting tract. During this time, the pollen tube responds to positional guidance cues that attract the tube to an unfertilized ovule (Chae and Lord 2011; Palanivelu and Tsukamoto 2012; Higashiyama and Yang 2017), where it penetrates synergid cells, ruptures, and releases the two sperm cells. Sperm cells fuse with the egg and central cells to produce a new embryo and the surrounding endosperm tissue, respectively.

Pollen tubes respond to numerous positional guidance cues during different points along their journey to unfertilized ovules. In the transmitting tract, pollen tubes follow a gradient of gamma aminobutyric acid (GABA) and are additionally provided with other attractants and nutrients in this structure (Palanivelu et al. 2003). Closer to the ovule, pollen tubes perceive ovule-secreted LURE peptides through the Pollen Receptor Kinase 6 (PRK6) receptor-like kinase that cause pollen tubes to re-orient growth toward the unfertilized ovule (Okuda et al. 2009; Takeuchi and Higashiyama 2016). Rapid Alkalinization Factor (RALF) peptides, which are perceived by *Catharanthus roseus* Receptor-Like Kinase (CrRLK) receptor complexes, also play a role in regulating the process of pollen tube rupture once the pollen tube has

Communicated by Weicai Yang.

Kayleigh J. Robichaux and Devin K. Smith contributed equally to this work.

✉ Ian S. Wallace
iwallace@unr.edu

[1] Department of Biochemistry and Molecular Biology, University of Nevada, Reno, 1664 N. Virginia St. MS0330, Reno, NV 89557, USA

Published online: 24 May 2023

reached the synergid cells (Ge et al. 2017, 2019). While the chemical nature of these attractants and their associated molecular mechanisms are coming into view, mechanical signaling and the modulation of cell adhesion or cell–cell signaling that occurs during the pollen tube trajectory through the female tissues is still poorly understood.

Pollen–pistil interactions represent a unique system to investigate signaling processes associated with cell adhesion, cell–cell interactions, and cell-to-cell communication in plants. Most other cells in the plant body are cemented to neighboring cells early in development through cell wall extracellular matrices. Vegetative plant cells are proposed to adhere to one another through extensive contacts within their cell walls that are largely mediated by pectic polysaccharides in the middle lamella, and these contacts are proposed to largely remain stable throughout the life of the plant (Daher and Braybrook 2015; Behar et al. 2017). In contrast, pollen tubes interact with multiple cell types, including stigmatic papillae, cells of the stigma–style interface, the transmitting tract, and the ovule during pollen tube growth through the pistil (Johnson et al. 2019; Robichaux and Wallace 2021), suggesting that the pollen tube must modulate cell adhesion and cell–cell interactions as it traverses the pistil. Additionally, the pollen tube experiences vast pressure differences during this trajectory. For example, pollen tubes must initially penetrate the stigmatic papillar cells by elongating between the cuticle and cell wall of these cells (Ndinyanka Fabrice et al. 2017; Riglet et al. 2020), grow through the apoplastic space in tightly packed cells within the stigma tissue, and finally emerge into the less densely packed transmitting tract. The changes in cellular turgor pressure imposed on the pollen tube by these growth parameters would destroy normal cells (Nezhad et al. 2013; Yanagisawa et al. 2017), and recent work has demonstrated that a signaling pathway composed of RALF4 and the BUDDHA'S PAPER SEAL1/2 (BUPS1/2) CrRLK receptors actively prevents premature bursting of pollen tubes during these extremes of cellular pressure (Zhou et al. 2021). Despite these advances, the mechanical signaling that facilitates pollen tube growth through the female reproductive tract remains largely unclear.

We previously demonstrated that disruption of the Arabidopsis *O-FUCOSYLTRANSFERASE1 (OFT1)* gene, a glycosyltransferase with sequence similarity to metazoan protein *O*-fucosyltransferases, resulted in a nearly 2,000-fold reduction in pollen transmission efficiency in pollen outcrosses from a heterozygous plant, and a ten-fold decrease in seed set in homozygous plants due to compromised pollen tube penetration through the stigma–style interface (Smith et al. 2018b). Therefore, we postulate that OFT1 may regulate aspects of mechanical signaling during pollen tube penetration (Smith et al. 2018a). Here, a forward genetic screen was conducted to identify Suppressor of OFT (SOFT) mutants with the hypothesis that these suppressor mutants could identify genetic interactors of OFT1 that inform on its function. Among the mutants identified in this screen was *soft2*, which presented with partially restored seed set, silique length, pollen tube penetration, and pollen transmission phenotypes associated with the parent *oft1* mutant. The causative genetic lesion in the *soft2-1* mutant was mapped to an EMS-induced stop codon in AtGAUT14, an enzyme that synthesizes pectic homogalacturonan (HG) in the pollen tube cell wall. Thus, this genetic relationship suggests that disruption of HG synthesis might allow *oft1* pollen tubes to enhance their penetrative ability in the pistil, suggesting that specific cell wall structural features play a role in pollen tube invasion through the stigma–style interface.

Results

Soft mutant screen and description of the soft2 mutant

Previously, we demonstrated that loss-of-function mutations in the Arabidopsis *O-FUCOSYLTRANSFERASE1 (OFT1)* gene cause decreased pollen tube penetration through the stigma–style interface that led to decreased seed set, reduced silique length, and vastly decreased pollen transmission efficiency (Smith et al. 2018b). Although AtOFT1 bears weak amino acid sequence similarity to metazoan protein *O*-fucosyltransferases, the precise biochemical function of this enzyme is unknown. Thus, we postulated that identifying genetic modifiers of *oft1* mutants might shed light on the genetic basis of pollen tube penetration defects in this mutant. To examine this hypothesis, we performed a forward genetic screen to identify suppressor mutations that improve *oft1* mutant fertility. Homozygous *oft1-3* mutant seed was subjected to EMS mutagenesis, and the resulting M1 seed was grown to reproductive maturity. Approximately 10,000 M1 plants were screened for increased silique size as a visual assay for *oft1* suppression, and this approach led to the identification of multiple suppressor mutants, including the *soft2* mutant.

soft2-1;oft1-3 mutants exhibited silique lengths that were 56% longer than *oft1-1* and 63% longer than *oft1-3* homozygous mutants (Fig. 1A and 1B). However, *soft2-1;oft1-3* mutant silique lengths were 23% shorter than corresponding wild-type Col-0 controls, suggesting that the *soft2-1* mutation does not completely restore wild-type silique morphology. We additionally assessed seed set in the *soft2-1;oft1-3* mutant compared to *oft1* and Col-0 controls (Fig. 1C and 1D). Seed set in *soft2-1;oft1-3* mutants increased 6 and 5.8-fold compared to *oft1-1* and *oft1-3* mutant alleles, but was only 70% of wild-type Col-0 controls (Fig. 1D), again suggesting that the *soft2-1* mutation partially suppresses

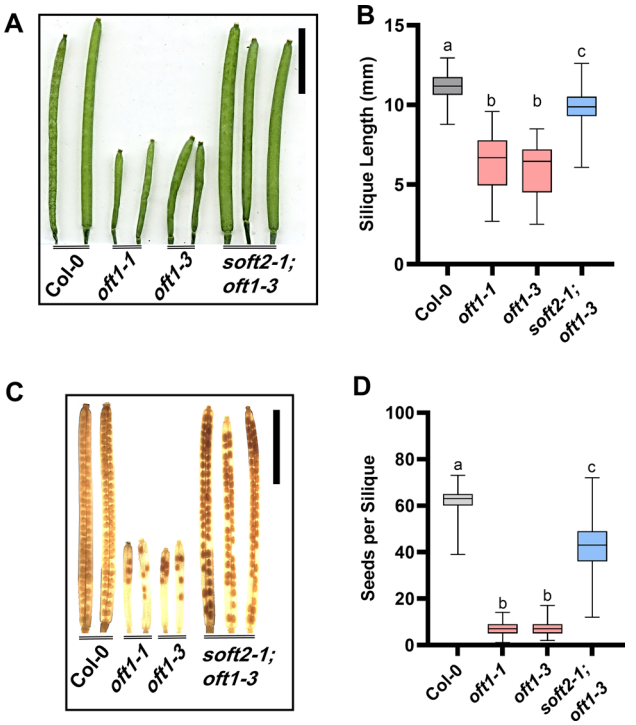

Fig. 1 Silique morphology and seed set of the *soft2-1* suppressor mutant: mature siliques were collected from six-week-old wild-type Col-0, *oft1-1*, *oft1-3*, and *soft2-1;oft1-3* plants. **A** Representative images of siliques collected from these genotypes are shown. **B** Quantification of silique lengths for wild-type Col-0 (gray box), *oft1-1* and *oft1-3* (red boxes), and *soft2-1;oft1-3* (blue box) ($n = 76–206$). **C** Mature siliques were removed and cleared in 70% ethanol as described in Materials and Methods to visualize seed set. **D** Quantification of seed set in wild-type Col-0 (gray box), *oft1-1, oft1-3 (*red boxes), and *soft2-1;oft1-3* (blue box) ($n = 82–205$). Scale bars in **A** and **C** represent 2 mm. For **B** and **D**, the center line in each box represents the median, and edges of the box represent 1st and 3rd quartiles. Error bars represent minimum and maximum values. In **B** and **D**, statistical significance was analyzed by one-way ANOVA and Tukey's HSD post hoc analysis. Letters above samples indicate significantly different groups ($P < 0.0001$)

the seed set phenotypes of *oft1* mutants. Overall, these results suggest that *soft2-1* is a partial suppressor of *oft1* and that this mutation may increase the competitiveness of *soft2;oft1-3* pollen compared to the original *oft1* mutant parent.

Mapping of soft2 candidate mutations

To identify the causative locus associated with the *soft2-1* mutation, a mapping by sequencing approach was taken. The *soft2-1* mutant was generated in the *oft1-3* background, and the *soft2-1;oft1-3* mutant was backcrossed to *oft1-1* to remove mutations associated with the *oft1-3* background. The resulting F1 progeny were grown to the reproductive stage, and plants with large siliques were genotyped to verify the presence of both *oft1* T-DNA insertions. Genomic DNA was isolated from thirty segregating F1 plants meeting these criteria, and the pooled genomic DNA samples were subjected to Illumina sequencing to identify candidate single nucleotide polymorphisms (SNPs) that co-segregate with the *soft2* phenotype.

This approach revealed a peak of preferentially co-segregating SNPs on chromosome 5 (Supplemental Fig. 1A), which could be narrowed to an interval of approximately 1 Mb based on SNP frequency. We filtered SNPs in this interval for G to A or C to T mutations, which are consistent with the EMS mechanism and used SnpEff (Cingolani et al. 2012) to predict the functional outcomes associated with EMS-induced mutations in this interval. This approach narrowed the number of candidates to 13 genes that contained missense or nonsense mutations that were consistent with EMS mutagenesis in this interval (Supplemental Table I). Finally, we surveyed potential candidate mutations for their expression in reproductive tissues (Supplemental Fig. 1B). Based on these criteria, the most likely candidate *soft2-1* mutation was a W448 to stop mutation in the *GALACTURONOSYLTRANSFERASE14 (GAUT14)* gene (Fig. 2A). GAUT14 is a HG: galacturonosyltransferase that participates in pectic HG synthesis (Engle et al. 2022). Prior work has also demonstrated that this protein is highly expressed in pollen and germinating pollen tubes, where GAUT14, along with the closely related GAUT13, is essential for pollen tube HG synthesis and pollen tube elongation (Wang et al. 2013a). Therefore, these results suggest that a loss-of-function mutation in GAUT14 is likely responsible for the *soft2* suppression effect.

To confirm this hypothesis, we crossed the *oft1-3* mutant with the previously described *gaut14-1* T-DNA null mutant (Wang et al. 2013a) (Fig. 2A). We first assessed silique length and seed set phenotypes of the resulting *oft1-3;gaut14-1* double mutant, which were virtually identical to the original *soft2-1;oft1-3* mutant. Quantification of silique lengths (Fig. 2B and 2D) and seed set (Fig. 2C and 2E) demonstrate that *soft2-1;oft1-3* and *oft1-3;gaut14-1* plants produce significantly longer siliques than those of the *oft1* mutant background. Although silique length is not completely restored to wild type in the *oft1-3;gaut14-1* double mutant, the *oft1* mutant silique length is partially suppressed, resulting in an intermediate phenotype between *oft1* and wildtype phenotypes. This pattern is also seen in seed set quantification (Fig. 2C and 2E), which again show this partial restoration to wildtype phenotype when the *oft1* mutation is present in combination with the *soft2-1* mutation in *GAUT14*. Ultimately, these data confirm that *gaut14* disruption is the causative genetic disruption underlying *soft2*.

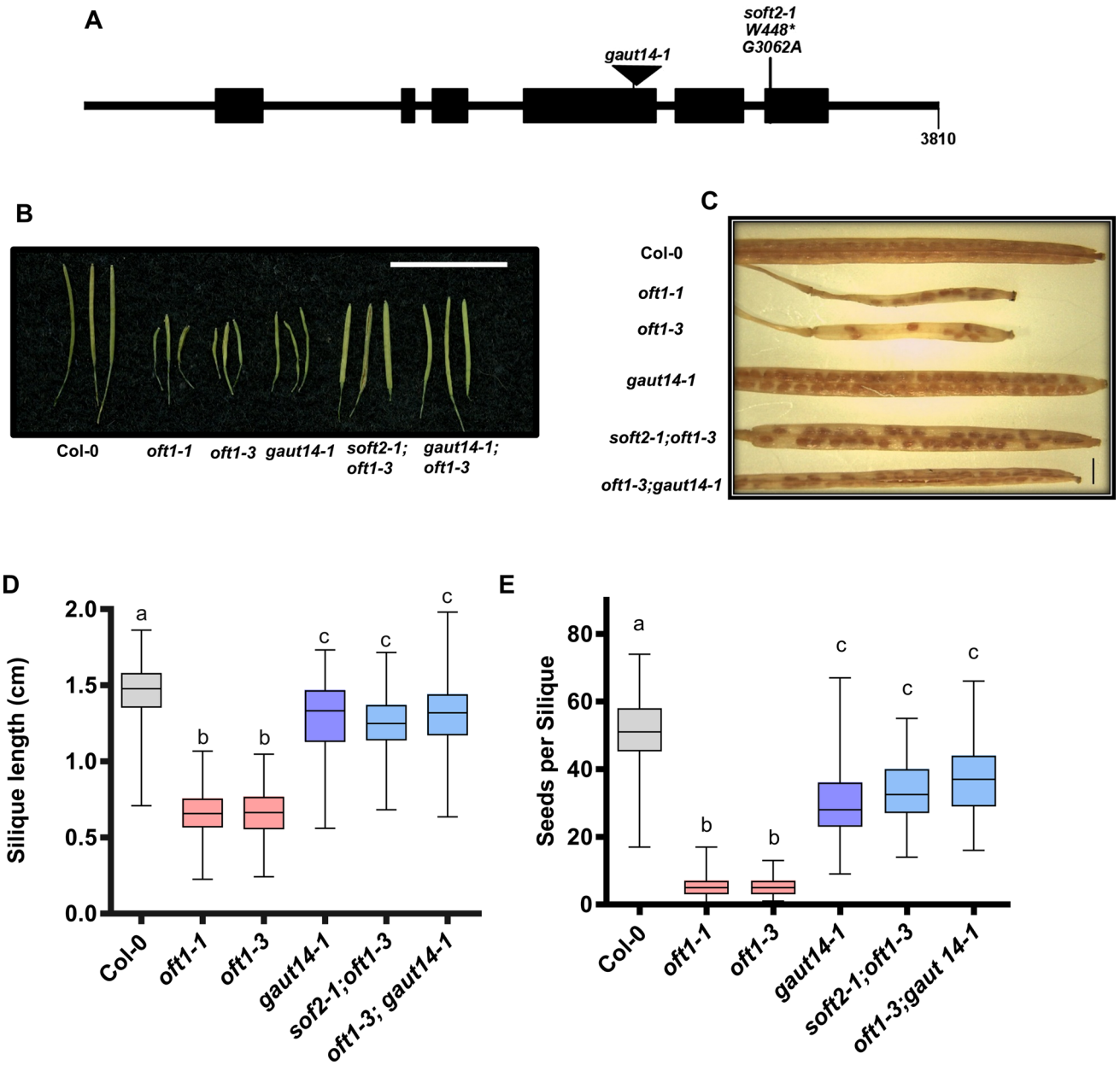

Fig. 2 Mutations in Arabidopsis GAUT14 are responsible for the *soft2-1* phenotype: **A** The gene structure of Arabidopsis GAUT14 (At5g15470) is shown with the positions of the *soft2-1* EMS and *gaut14-1* T-DNA mutations shown. Siliques were collected from six-week-old Arabidopsis plants of the indicated genotypes. Representative siliques **B** and seed set **C** images are shown for indicated genotypes. Scale bars in B and C are 20 mm and 1 mm, respectively. Silique length **D** and seed set **E** were quantified for the indicated genotypes. For box plots in **D** and **E**, the central line represents the median value, borders of the boxes represent the 1st and 3rd quartile, and error bars represent minimum and maximum values ($n = 217–642$ for D and 72–261 for E). Statistical analysis was performed with one-way ANOVA followed by Tukey's HSD post hoc analysis. Letters above samples indicate significantly different groups ($P < 0.0001$)

Soft2 suppresses various reproductive phenotypes associated with the oft1 mutant

Our prior work indicated that *oft1* mutant pollen exhibits a nearly 2000-fold decrease in pollen transmission efficiency (Smith et al. 2018b), so we sought to investigate how *gaut14* mutations impact this parameter. Pollen outcrosses from various genotypes indicated in Table 1 were performed using *MALE STERILE1* (*MS1*) mutants (Wilson et al. 2001), and surprisingly, *oft1-1* or *oft1-3* heterozygous pollen transmitted slightly better that was previously reported for Col-0 pistils (Smith et al. 2018b). Despite this small increase in pollen tube transmission compared to Col-0, *oft1* mutant pollen was still extremely compromised in their ability to

Table 1 Pollen transmission efficiency measurements:

Parents (♀x♂)[a]	#R[b]	#S[b]	Total	TE[c]	%R	% Expected[d]	*P* value
ms1 × *oft1-1*$^{\pm}$	3	864	867	0.35	0.35	50	$P<0.0001$
ms1 × *oft1-3*$^{\pm}$	2	702	704	0.28	0.28	50	$P<0.0001$
ms1 × *soft2-1*$^{\pm}$;*oft1-1*$^{\pm}$	23	389	412	5.91	5.58	0.35	$P<0.0001$
ms1 × *soft2-1*$^{\pm}$;*oft1-3*$^{\pm}$	47	691	738	6.80	6.37	0.28	$P<0.0001$
ms1 × *oft1-3*$^{\pm}$;*gaut14-1*$^{-/-}$	147	1460	1607	10.1	10.1	0.28	$P<0.0001$

[a]Parent lines of each cross are shown

[b]The number of progeny that were resistant (#R) or sensitive (#S) to the T-DNA-associated herbicide marker is shown. *Oft1-3* progeny were scored on media containing BASTA, while *oft1-1* seedlings were selected on media containing kanamycin

[c]The transmission efficiency (TE) of each cross was calculated as #R/#S × 100

[d]The expected segregation ratio for each outcross is shown. For crosses containing the suppressor mutation, the transmission efficiency of the corresponding *oft1* mutant parent was used as the expected value

fertilize, displaying transmission efficiencies of 0.35% (*oft1-1*) and 0.28% (*oft1-3*) which is far below the expected 50%. We then used these transmission efficiencies as a baseline to investigate how well the *soft2-1* or *gaut14-1* mutations suppress the *oft1* pollen transmission defect. *soft2-1*$^{\pm}$;*oft1-1*$^{\pm}$ and *soft2-1*$^{\pm}$;*oft1-3*$^{\pm}$ pollen were first outcrossed to *ms1* pistils, and the transmission efficiency of the *oft1* mutant allele was measured (Table 1). This experiment revealed that the presence of the *soft2-1* allele increased transmission efficiency of the *oft1-1* allele to 5.6% and the *oft1-3* allele to 6.3%, representing 16- and 22.5-fold increases in transmission efficiency compared to the parent *oft1* allele. We also outcrossed *oft1-3*$^{\pm}$;*gaut14-1*$^{-/-}$ pollen to *ms1* pistils and found that transmission efficiency increased to 10.1%, representing a 33-fold increase in pollen transmission efficiency. Thus, these results suggest that multiple mutations in *GAUT14* partially rescue the pollen tube transmission efficiency defects associated with *oft1* mutants and increase pollen tube transmission efficiency by between 16- and 33-fold.

To expand upon which *oft1* mutant phenotypes might be suppressed by mutation of *GAUT14*, semi-in vivo assays (see Materials and Methods) were used to quantify pollen tube penetration through the stigma–style interface using different pollen tube genotypes. Col-0, *oft1-3*, *gaut14-1*, and *oft1-3;gaut14-1* plants were grown to reproductive maturity, and pollen from these plants was applied to respective, emasculated *ms1* pistils. The pollen germinated on the pistils for 30 min, and the pollinated *ms1* pistils were dissected and placed on an agarose pad for imaging. Images of emerging pollen tubes were collected at 2, 4, 6, and 8 h after pollination (HAP). By 4 HAP, there were visibly more Col-0, *gaut14-1*, and *oft1-3;gaut14-1* pollen tubes emerging from the stigma–style interface compared to *oft1-3* pollen tubes (Fig. 3A). At 8 HAP, there was a threefold to fourfold increase in pollen tube emergence when comparing *oft1-3* pollen tubes to Col-0, *gaut14-1*, and *oft1-3;gaut14-1* (Fig. 3B). Similar results were obtained for the *soft2-1; oft1* EMS mutant (Supplemental Fig. 2), suggesting that both mutant alleles exhibited increased pollen tube penetration through the stigma–style interface. Lengths of pollen tubes growing through each individual pistil ($n=10$) per genotype were measured over time to produce pollen tube growth rates through *ms1* pistils (Fig. 3C). There was no difference in growth rate between *gaut14-1* and *oft1-3;gaut14-1* pollen, but both of these genotypes were found to have a significantly higher growth rate when compared to *oft1-3* pollen. These data demonstrate that mutation of *GAUT14* in the *oft1* mutant background partially restores the ability of mutant pollen to penetrate through pistil tissue.

Discussion

The major goal of this study was to identify genetic modifiers of the *oft1* mutant, which is compromised in pollen tube penetration through the stigma–style interface, leading to severe pollen tube transmission deficiencies, reduced silique length, and reduced seed set (Smith et al. 2018b). We EMS mutagenized *oft1* plants and performed a forward genetic screen to identify Suppressor of OFT (SOFT) mutants and mapped the causative genetic lesion of the *soft2-1* mutant to a W448* mutation in the *GALACTURONOSYLTRANSFERASE14* (*GAUT14*) gene. Both *oft1-3;soft2-1* and *oft1-3*;*gaut14-1* double mutants exhibited increased silique elongation, seed set, pollen transmission, and pollen penetration through the stigma–style interface compared to the parent *oft1-3* mutant. In the case of all these phenotypes, the *oft1-3;soft2-1* or *oft1-3;gaut14-1* pollen tubes did not perform as well as wild type, suggesting that the *GAUT14* mutation confers partial suppression of these phenotypes.

Plant cell walls are complex extracellular matrices that consist of multiple polysaccharide networks, including cellulose, neutral hemicelluloses, and acidic pectins. Pectic polysaccharides consist of multiple subdomains, including

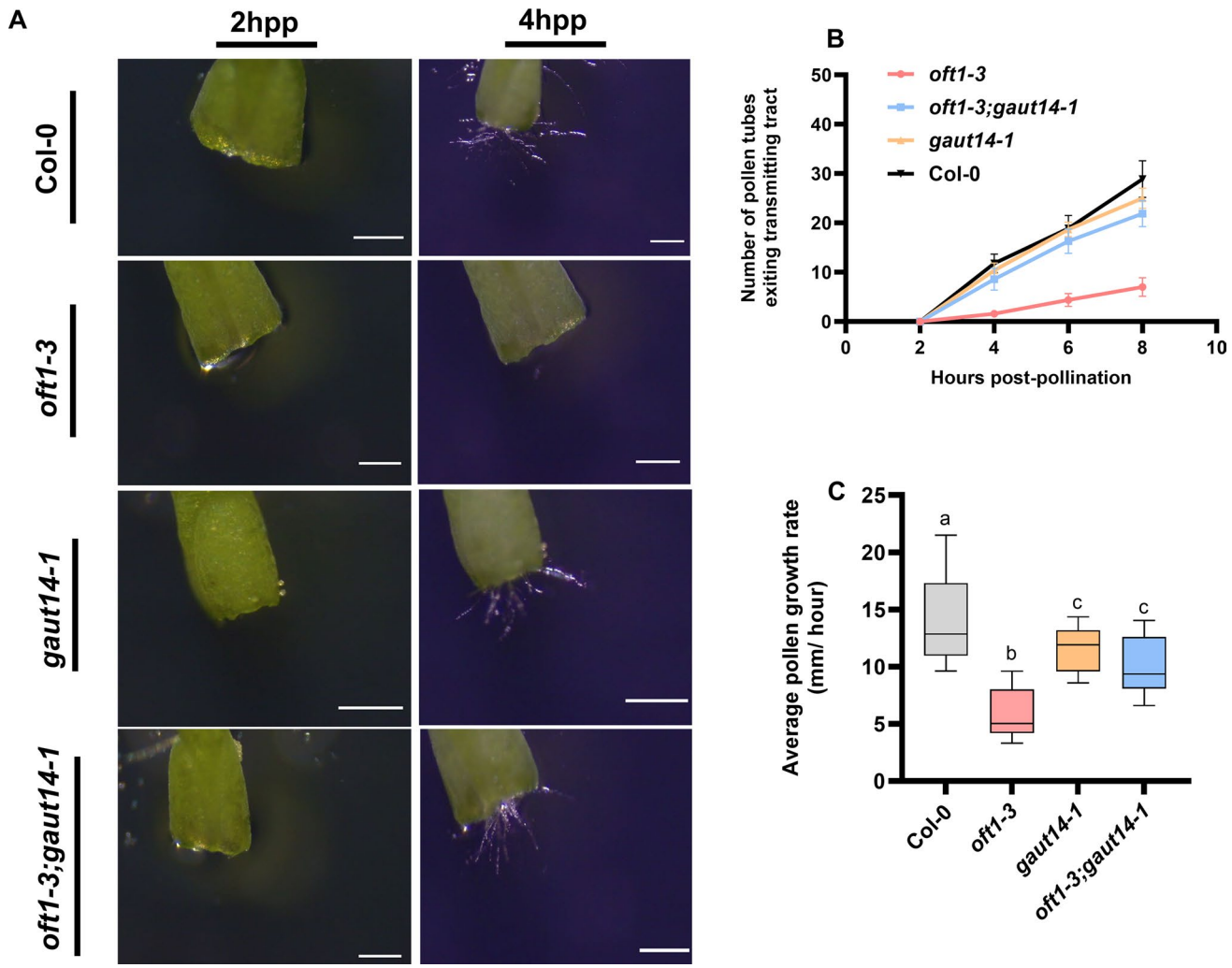

Fig. 3 Semi-in vivo analysis of pollen tube penetration: Pollen was harvested from reproductively mature flowers of 6-week-old plants from the indicated genotype and used to pollinate *ms1* pistils. Pollinated pistils were dissected after pollination and visualized for pollen tube emergence as described in Materials and Methods. **A** Visual comparison of representative semi-in vivo *ms1* pistils pollinated with pollen from the indicated genotype and imaged at 2- and 4-h time points (scale bar represents 0.5 mm). **B** The number of pollen tubes exiting the transmitting tract over an 8-h time course was quantified for *ms1* pistils pollinated with pollen from the indicated genotype. Error bars represent SEM ($n = 10$). **C** Growth rates for pollen tubes of the indicated genotype emerging from *ms1* cut pistils were calculated from SIV images as described in Materials and Methods. For box plots, the median value is indicated by the center line, while the perimeter of the box represents the first and third quartile. Error bars represent minimum and maximum values ($n = 10$). Statistical analysis was performed with one-way ANOVA followed by Tukey's HSD post hoc analysis. Letters above samples indicate significantly different groups ($P < 0.001$).

HG, rhamnogalacturonan-I (RG-I), and rhamnogalacturonan-II (RG-II) (Caffall and Mohnen 2009). Prior work has indicated that GAUT14 is a robust HG: galacturonosyltransferase that is localized to the Golgi apparatus in growing pollen tubes, and that this protein participates in the synthesis of HG redundantly with GAUT13 (Wang et al. 2013a; Engle et al. 2022). Indeed, *gaut13;gaut14* double mutants exhibited reduced pollen tube elongation, swelling and bursting of the pollen tube, and poor penetration of pollen tubes through the reproductive tissues (Wang et al. 2013a). We endeavored to generate *oft1;gaut13* double mutants to understand whether the suppression effect was specific to GAUT14, but unfortunately, these genes are tightly linked on the same chromosome, which prevented functional characterization of a double homozygous line. Still, it is curious that *gaut14* mutations alone are sufficient to suppress *oft1*-induced fertility defects, suggesting that GAUT13 and GAUT14 are not completely redundant and may have some unique functions. We also note that *gaut14-1* individual mutants exhibited reduced seed set, which was a previously unidentified phenotype of this mutant. Previous work indicated that *gaut14* mutations alone were not sufficient to elicit reduced

transmission of mutant pollen, suggesting that *GAUT14* may participate in some aspect of pollen–pistil interactions in female tissues, but this phenotype is independent of *oft1* suppression. Prior enzymatic characterization of GAUT13 and GAUT14 revealed that while both of these enzymes robustly synthesize HG, GAUT14 has a nearly four-fold higher HG synthesis activity in the presence of a short HG oligomer compared to GAUT13 (Engle et al. 2022). This observation may indicate that GAUT14 is responsible for the synthesis of unique domains of elongated HG in the pollen tube, and that in *oft1* pollen tubes, the precise HG glycans synthesized by GAUT14 contribute to the reduction in pollen tube penetration.

There is also increasing evidence that enzymes related to OFT1 directly participate in the synthesis of pectic polysaccharide domains. The Arabidopsis genome contains approximately 40 genes that are annotated as putative protein *O*-fucosyltransferases (Smith et al. 2018b; Takenaka et al. 2018), and AtOFT1 is a member of this large gene family. Although the precise biochemical functions for many of these genes remain unclear, it is likely that this gene family represents a diversity of glycosyltransferase activities. Recent work has demonstrated that a subgroup of these proteins are actually RG-I Rhamnosyltransferase (RRT) enzymes that catalyze one of the essential reactions in the production of pectic RG-I (Takenaka et al. 2018). Other work has shown that MANNAN SYNTHESIS-RELATED 1/2 (MSR1/2) plays an undefined role in regulating and activating Cellulose Synthase-Like A glycosyltransferases that catalyze cell wall mannan biosynthesis (Wang et al. 2013b; Voiniciuc et al. 2019; Robert et al. 2021), again suggesting a diversity of glycosyltransferase activities in the putative POFT family. Thus, these observations and our work described here suggest that OFT1 may be either indirectly participating in pollen tube cell wall deposition by regulating enzymes that synthesize cell wall polysaccharides or that OFT1 is actually a cell wall-synthesizing glycosyltransferase.

We propose two potential models to explain these findings. First, it is possible that AtOFT1 is a protein *O*-fucosyltransferase that glycosylates and regulates the binding of an unidentified receptor to cell wall pectic components (Fig. 4). Candidates for such a receptor could include the CrRLK family of receptors because these receptors bind pectic polysaccharides in addition to various RALF peptides (Lin et al. 2022; Tang et al. 2022), and some members of this family have been implicated in mechanical signaling at the stigma–style and transmitting tract interface during pollen tube growth through the pistil (Zhou et al. 2021). In this model, *oft1* mutants might exhibit dysregulated receptors that initiate inhibitory signaling cascades leading to reduced pollen tube growth. The additional *soft2/gaut14* mutations in this background may mediate suppression by altering pectin fine structure in the pollen tube and destroying the signal that is recognized by the receptor. An alternative model is that AtOFT1 and GAUT14 reciprocally regulate the fine structure of the pollen tube cell wall leading to reciprocal changes in wall stiffness. *oft1* pollen tubes may fail to penetrate the stigma–style interface due to increased pollen wall stiffness through an unclear mechanism, while a second *gaut14* mutation passivates the pollen tube cell wall facilitating pollen tube elongation. While the mechanistic interplay between AtOFT1 and GAUT14 remains unclear, in this study, we have demonstrated that two independent *gaut14* mutations suppress the phenotypes of the *oft1* mutant. This work shows that there is a clear genetic relationship between fine pectin structure, pollen tube penetration, and the biological function of AtOFT1 that are interdependent and mediate complex signaling and mechanical processes required for successful fertilization events to occur.

Materials and methods

Plant growth and maintenance

Arabidopsis thaliana seeds were sterilized in seed sterilization solution (3% [v/v] sodium hypochlorite, 0.1% [w/v] sodium dodecylsulfate) for 20 min at 25 °C. Seeds were washed 5 times with sterile water and stratified at 4 °C for 48 h prior to plating. Seeds were germinated on Murashige and Skoog (MS) medium (1/2X MS salts, 10 mM MES-KOH pH 5.7, 1% [w/v] sucrose, 1% [w/v] phytoagar) and grown vertically for 7 days under long-day conditions (16-h light/8-h dark) at 24 °C. Seedlings were then transferred to soil and propagated in a Percival AR-66L2 growth chamber under long-day conditions until seed set.

For silique length measurements and seed set imaging, siliques were harvested from 6-week-old reproductively mature plants and placed on an Epson Perfection V550 Scanner with an internal scale for size reference. Silique lengths were measured using ImageJ software (imagej.nih.gov/ij). After imaging, siliques were incubated for 5 days in 70% [v/v] ethanol at 25 °C. Seeds in the cleared siliques were visualized with a Leica EZ4HD dissecting microscope at 40X magnification.

Bulk segregant analysis for mutant mapping

High molecular weight genomic DNA was extracted from siliques of *soft2-1;oft1* mutants using the Qiagen DNeasy Plant Mini Kit (Qiagen) according to the manufacturer's instructions. DNA concentrations were quantified using PicoGreen dsDNA quantification reagent (ThermoFisher).

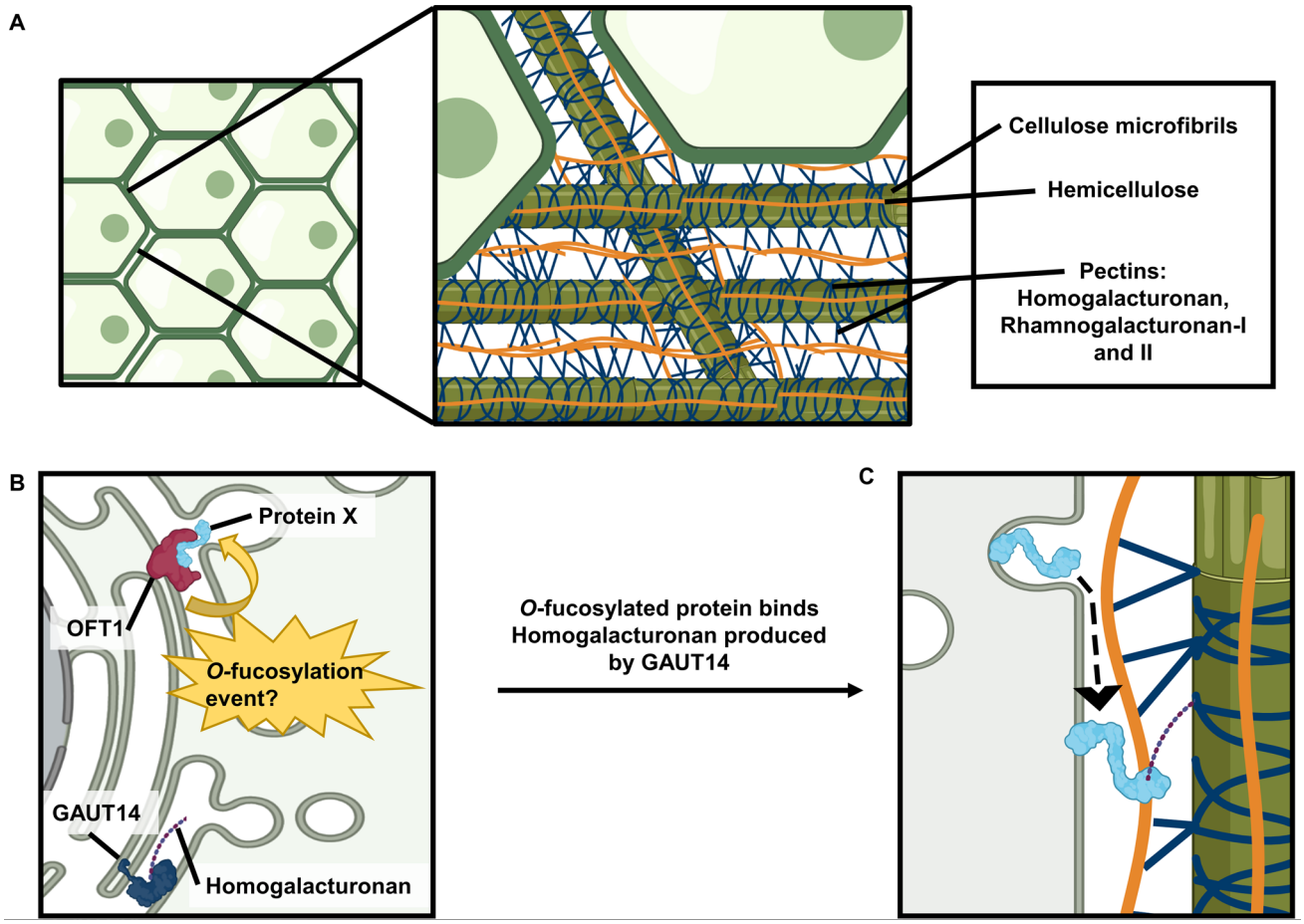

Fig. 4 Schematic of proposed OFT1 enzymatic relationship to GAUT14 activity. **A**. A magnified view of cell wall components at the middle lamella between two cells is shown. **B** The proposed sequence of enzyme activity is shown in the Golgi apparatus. GAUT14 polymerizes α-(1→4)-linked-*D*-galacturonic acid, while OFT1 is *O*-fucosylating an unknown target protein. **C** The OFT1 acceptor molecule specifically binds the homogalacturonan product generated by GAUT14, thus impacting cell wall integrity and/or mechanistic signaling

The resulting genomic DNA samples were sheared to a size distribution of 500–800 bp using a CovarisM220 focused ultrasonicator, and the size distribution was examined using an Agilent 2100 BioAnalyzer system. Sheared genomic DNA libraries were labeled with unique Illumina barcode tags and sequenced using a NextSeq 500 Mid Output v2 flowcell on an Illumina NextSeq 500 instrument in the Nevada Genomics Center.

The resulting sequencing data were first processed to remove Illumina adapters and low-quality sequence elements using Trimmomatic (Bolger et al. 2014). Trimmed reads were aligned to the TAIR10 Arabidopsis thaliana genome using the Burrows-Wheeler Aligner algorithm (Li and Durbin 2009). Single nucleotide polymorphism (SNP) and indel variants were called using SAMtools (Li et al. 2009; Li and Barrett 2011) and analyzed using BCFTools. The frequencies of SNP events were used to identify an over-represented genomic interval containing the causative mutation, and each EMS-type SNP in this interval was analyzed using snpEff (Cingolani et al. 2012) to determine potential effects on target genes.

SIV assays

Mature anthers from 6-week-old Arabidopsis plants (Col-0, *oft1-3*, *gaut14-1*, and *oft1-3;gaut14-1*) were dissected and used to pollinate *ms1* pistils. Thirty minutes after pollination, pollinated *ms1* pistils were dissected from the parent plant using forceps and transferred to a pollen germination medium (PGM; 5 mM $CaCl_2$, 0.01% H_3BO_3, 5 mM KCl, 1 mM $MgSO_4$, 10% [w/v] sucrose, and 1.5% [w/v] low-melting-point agarose, pH 7.8)-agarose pad on a microscope slide after allowing to cool to 25° C. The dissected, pollinated stigmas were incubated in a dark, humidified chamber at 25° C for the indicated time. Pollen tube growth through stigmatic tissue was imaged using a Leica EZ4HD

Dissecting microscope at 35X magnification. After each set of images was collected for a given time point, the samples were returned to the humidified chamber in the dark until the next images were collected. Pollen tube lengths were measured by an internal scale and ImageJ software.

Genotyping

Genomic DNA was extracted from Arabidopsis plants as previously described (Villalobos et al. 2015). Genomic DNA samples were subjected to PCR genotyping using ExTaq DNA polymerase (Takara Bio) with the following locus-specific primers: *gaut14-1* (SALK_000091 LP: AAACAT TTGCTCTTGTGCTGC; SALK_000091 RP: TTAAAC GCTTTGACATCACCC), *oft1-3* (WiscDsLox489-492M4 LP: GTGAACCGCAACAAAAGGTAC; WiscDsLox489-492M4 RP: ATTTGCATGTCAAGTTCGAGG). T-DNA left border regions were amplified with an insertion-specific left border primer (LBb1.3: ATTTTGCCGATTTCGGAA C; WiscDsLox LB: AACGTCCGCAATGTGTTATTAAGT TGTC) and the gene-specific right primer (RP) indicated above. Reactions were cycled under the following conditions: 95 °C initial denaturation time for 5 min, 35 cycles of 95 °C (30 s), 52 °C (30 s), and 72 °C (1.5 min) and a final extension at 72 °C for 7 min. The resulting PCR products were separated on 1% (w/v) agarose gels and documented using a Bio-Rad Gel Doc XR + workstation.

Author contribution statement KJR, DKS, MNB, CW, JFH, and ISW conceived of the research and performed experiments. ISW, KJR, and JFH wrote the manuscript with editing input from MNB and DKS. ISW, DKS, and JFH obtained funding for the research.

Supplementary Information The online version contains supplementary material available at https://doi.org/10.1007/s00497-023-00468-5.

Acknowledgements We would like to thank Dr. Gloria Atmodjo and Dr. Debra Mohnen (University of Georgia Complex Carbohydrate Research Center) for kindly providing *gaut14-1* seed. This work was funded by a National Science Foundation award (IOS-1947741), a National Science Foundation Graduate Research Fellowship to DKS, and National Science Foundation awards (IOS 1656774 and IOS 2129234) to JFH.

References

Behar H, Brenner N, Ariel G, Louzoun Y (2017) The middle lamella—more than a glue. Phys Biol 14:015004. https://doi.org/10.1088/1478-3975/AA5BA5

Bolger AM, Lohse M, Usadel B (2014) Trimmomatic: a flexible trimmer for Illumina sequence data. Bioinformatics 30:2114–2120. https://doi.org/10.1093/BIOINFORMATICS/BTU170

Caffall KH, Mohnen D (2009) The structure, function, and biosynthesis of plant cell wall pectic polysaccharides. Carbohydr Res 344:1879–1900. https://doi.org/10.1016/J.CARRES.2009.05.021

Chae K, Lord EM (2011) Pollen tube growth and guidance: Roles of small, secreted proteins. Ann Bot 108:627–636

Cingolani P, Platts A, Wang LL et al (2012) A program for annotating and predicting the effects of single nucleotide polymorphisms, SnpEff: SNPs in the genome of Drosophila melanogaster strain w1118; iso-2; iso-3. Fly 6:80–92. https://doi.org/10.4161/FLY.19695/SUPPL_FILE/KFLY_A_10919695_SM0001.ZIP

Daher FB, Braybrook SA (2015) How to let go: pectin and plant cell adhesion. Front Plant Sci 6:523. https://doi.org/10.3389/FPLS.2015.00523/BIBTEX

Engle KA, Amos RA, Yang JY et al (2022) Multiple Arabidopsis galacturonosyltransferases synthesize polymeric homogalacturonan by oligosaccharide acceptor-dependent or de novo synthesis. Plant J 109:1441–1456. https://doi.org/10.1111/TPJ.15640

Ge Z, Bergonci T, Zhao Y et al (2017) Arabidopsis pollen tube integrity and sperm release are regulated by RALF-mediated signaling HHS public access. Science 358:1596–1600. https://doi.org/10.1126/science.aao3642

Ge Z, Zhao Y, Liu MC et al (2019) LLG2/3 are co-receptors in BUPS/ANX-RALF signaling to regulate Arabidopsis pollen tube integrity. Curr Biol 29:3256-3265.e5. https://doi.org/10.1016/J.CUB.2019.08.032

Higashiyama T, Yang W (2017) Gametophytic pollen tube guidance: attractant peptides, gametic controls, and receptors. Plant Physiol 173:112. https://doi.org/10.1104/PP.16.01571

Johnson MA, Harper JF, Palanivelu R (2019) A fruitful journey: pollen tube navigation from germination to fertilization. Ann Rev Plant Biol 70:809–837. https://doi.org/10.1146/annurev-arplant-050718-100133

Li H, Barrett J (2011) A statistical framework for SNP calling, mutation discovery, association mapping and population genetical parameter estimation from sequencing data. Bioinformatics 27:2987–2993. https://doi.org/10.1093/BIOINFORMATICS/BTR509

Li H, Durbin R (2009) Fast and accurate short read alignment with Burrows-Wheeler transform. Bioinformatics 25:1754–1760. https://doi.org/10.1093/BIOINFORMATICS/BTP324

Li H, Handsaker B, Wysoker A et al (2009) The sequence alignment/map format and SAMtools. Bioinformatics 25:2078–2079. https://doi.org/10.1093/BIOINFORMATICS/BTP352

Lin W, Tang W, Pan X et al (2022) Arabidopsis pavement cell morphogenesis requires FERONIA binding to pectin for activation of ROP GTPase signaling. Curr Biol 32:497-507.e4. https://doi.org/10.1016/J.CUB.2021.11.030

Ndinyanka Fabrice T, Kaech A, Barmettler G et al (2017) Efficient preparation of Arabidopsis pollen tubes for ultrastructural analysis using chemical and cryo-fixation. BMC Plant Biol. https://doi.org/10.1186/s12870-017-1136-x

Nezhad AS, Naghavi M, Packirisamy M et al (2013) Quantification of cellular penetrative forces using lab-on-a-chip technology and finite element modeling. Proc Natl Acad Sci U S A 110:8093–8098. https://doi.org/10.1073/pnas.1221677110

Okuda S, Tsutsui H, Shiina K et al (2009) Defensin-like polypeptide LUREs are pollen tube attractants secreted from synergid cells. Nature 458:357–361. https://doi.org/10.1038/nature07882

Palanivelu R, Tsukamoto T (2012) Pathfinding in angiosperm reproduction: pollen tube guidance by pistils ensures successful double fertilization. Wiley Interdiscip Rev Dev Biol 1:96–113

Palanivelu R, Brass L, Edlund AF, Preuss D (2003) Pollen tube growth and guidance is regulated by POP2, an arabidopsis gene that controls GABA levels. Cell 114:47–59. https://doi.org/10.1016/S0092-8674(03)00479-3

Riglet L, Rozier F, Kodera C et al (2020) KATANIN-dependent mechanical properties of the stigmatic cell wall mediate the pollen tube path in arabidopsis. Elife 9:1–21. https://doi.org/10.7554/ELIFE.57282

Robert M, Waldhauer J, Stritt F et al (2021) Modular biosynthesis of plant hemicellulose and its impact on yeast cells. Biotechnol Biofuels 14:1–17. https://doi.org/10.1186/S13068-021-01985-Z/FIGURES/7

Robichaux KJ, Wallace IS (2021) Signaling at physical barriers during pollen-pistil interactions. Int J Mol Sci 22:12230. https://doi.org/10.3390/IJMS222212230

Smith DK, Harper JF, Wallace IS (2018a) A potential role for protein O-fucosylation during pollen-pistil interactions. Plant Signal Behav 13:e1467687. https://doi.org/10.1080/15592324.2018.1467687

Smith DK, Jones DM, Lau JBR et al (2018b) A putative protein O-fucosyltransferase facilitates pollen tube penetration through the stigma–style interface. Plant Physiol 176:2804–2818. https://doi.org/10.1104/pp.17.01577

Takenaka Y, Kato K, Ogawa-Ohnishi M et al (2018) Pectin RG-I rhamnosyltransferases represent a novel plant-specific glycosyltransferase family. Nat Plants 4:669–676. https://doi.org/10.1038/s41477-018-0217-7

Takeuchi H, Higashiyama T (2016) Tip-localized receptors control pollen tube growth and LURE sensing in Arabidopsis. Nature 531:245–248. https://doi.org/10.1038/nature17413

Tang W, Lin W, Zhou X et al (2022) Mechano-transduction via the pectin-FERONIA complex activates ROP6 GTPase signaling in Arabidopsis pavement cell morphogenesis. Curr Biol 32:508-517.e3. https://doi.org/10.1016/J.CUB.2021.11.031

Villalobos JA, Yi BR, Wallace IS (2015) 2-fluoro-L-fucose is a metabolically incorporated inhibitor of plant cell wallpolysaccharide fucosylation. PLoS ONE 10: e0139091. https://doi.org/10.1371/journal.pone.0139091

Voiniciuc C, Dama M, Gawenda N et al (2019) Mechanistic insights from plant heteromannan synthesis in yeast. Proc Natl Acad Sci U S A 116:522–527. https://doi.org/10.1073/PNAS.1814003116/SUPPL_FILE/PNAS.1814003116.SAPP.PDF

Wang L, Wang W, Wang YQ et al (2013a) Arabidopsis galacturonosyltransferase (GAUT) 13 and GAUT14 have redundant functions in pollen tube growth. Mol Plant 6:1131–1148. https://doi.org/10.1093/mp/sst084

Wang Y, Mortimer JC, Davis J et al (2013b) Identification of an additional protein involved in mannan biosynthesis. Plant J 73:105–117. https://doi.org/10.1111/TPJ.12019

Wilson ZA, Morroll SM, Dawson J et al (2001) The Arabidopsis MALE STERILITY1 (MS1) gene is a transcriptional regulator of male gametogenesis, with homology to the PHD-finger family of transcription factors. Plant J 28:27–39. https://doi.org/10.1046/J.1365-313X.2001.01125.X

Yanagisawa N, Sugimoto N, Arata H et al (2017) Capability of tip-growing plant cells to penetrate into extremely narrow gaps. Sci Rep. https://doi.org/10.1038/s41598-017-01610-w

Zhou X, Lu J, Zhang Y et al (2021) Membrane receptor-mediated mechano-transduction maintains cell integrity during pollen tube growth within the pistil. Dev Cell 56:1030-1042.e6. https://doi.org/10.1016/J.DEVCEL.2021.02.030

Publisher's Note Springer Nature remains neutral with regard to jurisdictional claims in published maps and institutional affiliations.

Springer Nature or its licensor (e.g. a society or other partner) holds exclusive rights to this article under a publishing agreement with the author(s) or other rightsholder(s); author self-archiving of the accepted manuscript version of this article is solely governed by the terms of such publishing agreement and applicable law.